Journal of Solid State Chemistry **160,** 45–49 (2001)
doi:10.1006/jssc.2001.9182, available online at http://www.idealibrary.com on IDEAL®

Preparation, Crystal Structure, and Magnetic Studies of a New $Sr_7Re_4O_{19}$ Double Oxide and Its Relation to the Structure of $Ba_7Ir_6O_{19}$

K. G. Bramnik, H. Ehrenberg, and H. Fuess

Institute for Materials Science, Darmstadt University of Technology, Petersenstrasse 23,D-64287, Darmstadt, Germany

Received November 16, 2000; in revised form March 13, 2001; accepted March 26, 2001; published online May 30, 2001

The complex oxide $Sr_7Re_4O_{19}$ has been synthesized and its crystal structure was determined by X-ray diffraction powder data analysis (space group $C2/m$; $a = 13.6379(3)$ Å, $b = 5.6035(2)$ Å, $c = 10.3700(3)$ Å; $\beta = 98.348(2)^\circ$, $Z = 2$, $R_I = 0.018$, $R_P = 0.050$). The compound crystallizes in a new structure type, which can be derived from the $Ba_7Ir_6O_{19}$ structure by removing the Ir atoms from the middle octahedron of three face-sharing IrO_6 octahedra units. This change results in the infinite *cis*-bridged chains of the ReO_6 octahedra linked together by common corners. Each chain is connected with another one by the corner-sharing of each second ReO_6 octahedron. The 10- and 12-coordinated Sr atoms are situated between these infinite structure fragments. Magnetic properties of the $Sr_7Re_4O_{19}$ compound were studied by SQUID measurements. © 2001 Academic Press

INTRODUCTION

In contrary to the other alkali-earth elements, strontium containing ternary rhenium oxides with a rhenium oxidation state less than $+7$ were scarcely investigated. Three different compounds were described in this system. Moreover, one of the reported compounds, Sr_xReO_3, $x = 0.4$–0.5, was synthesized under extreme conditions such as high pressure and high temperature (50 kbar, 900°C) (1). Its crystal structure based on a three-dimensional network built of corner-sharing Re_2O_{10} units. Two other compounds were synthesized by a standard ceramic technique, subsolidus reaction of the precursor oxides, SrO and ReO_3, at high temperature. The recently reported $Sr_{11}Re_4O_{24}$ compound (2) (space group $I4_1/a$) with rhenium in a formal oxidation state of $+6.5$ can also be considered as a cation-deficient perovskite-distorted structure. The ReO_6 octahedra are rotated along the [110] axis by $\approx 45^\circ$, resulting in a distortion of the oxygen environment around the Sr atoms, occupying the other half of the positions in the *B*-cation sublattice, from an octahedron to an irregular eight-fold polyhedron. The rotation of ReO_6 octahedra forms two kinds of nonequivalent channels filled by *A*-cations. In the first one only $\frac{3}{4}$ of the *A* positions are occupied by Sr cations with 12-fold and 10-fold coordinations. The second one contains Sr atoms surrounded by eight oxygen atoms. $Sr_{11}Re_4O_{24}$ shows interesting magnetic properties and orders ferrimagnetically below 12 K. The complex oxide $Sr_3Re_2O_9$ with a composition similar to $Sr_7Re_4O_{19}$ has already been reported in the literature (3). $Sr_3Re_2O_9$ was suggested to be isostructural with $Ba_3Re_2O_9$ (4), which has a hexagonal perovskite-like structure based on a $9R(chh)_3$ close-packed stacking of the BaO_3 layers with Re atoms situated in the octahedral interstices. However the X-ray powder diffraction pattern of the $Sr_3Re_2O_9$ sample was not completely indexed, and its crystal structure was not refined. In the present investigation we describe the synthesis, crystal structure, and magnetic properties of the new compound $Sr_7Re_4O_{19}$.

EXPERIMENTAL

SrO and ReO_3 (STREM Chemicals, 99.9%) oxides were chosen as starting materials. SrO was obtained by the decomposition of $SrCO_3$ at 1000°C for 24 h in vacuum, 10^{-4} mbar. Seven moles of SrO and 4 mol of ReO_3 were thoroughly mixed, ground in an agate mortar under a dry argon atmosphere, and placed in an alumina crucible to avoid a reaction with the silica tube during annealing. To control the partial oxygen pressure during the synthesis a mixture of metallic Ni and NiO was used. This mixture was placed in another alumina crucible and sealed together with the sample in a silica tube with an 8–10 cm^3 volume at 10^{-3} mbar pressure. The raw material was annealed for 24 h at 800°C, which corresponds to a partial oxygen pressure value $p(O_2) = 1.02 \times 10^{-14}$ bar, which was established by the getter mixture of Ni/NiO in the balance state at this temperature. The sample was quenched after the synthesis.

X-ray diffraction data for the phase analysis and the crystal structure determination were collected with a STOE STADI/P powder diffractometer ($CoK\alpha_1$ radiation, curved Ge monochromator, transmission mode, step 0.02° (2θ), PSD counter). For structure refinements the RIETAN-97

0022-4596/01 $35.00

program (5) was used, based on the Rietveld method with a modified pseudo-Voigt profile function.

The electron diffraction (ED) investigations were performed using a Philips CM20 UT transmission electron microscope, operating at an accelerating voltage of 200 kV.

The magnetic properties of $Sr_7Re_4O_{19}$ were studied using a superconducting quantum interference device (SQUID) from Quantum Design in a temperature range from 4.5 to 300 K and a field strength up to 6.5 T.

RESULTS AND DISCUSSION

a. Structure Determination

The X-ray powder diffraction pattern of an annealed sample with a $Sr_7Re_4O_{19}$ bulk composition was completely indexed on the basis of a C-centered monoclinic cell with $a = 13.6379(3)$ Å, $b = 5.6035(2)$ Å, $c = 10.3700(3)$ Å; $\beta = 98.348(2)^\circ$. The symmetry was confirmed by electron diffraction.

Due to the similarity between the cell parameters of this compound and the already known compound $Ba_7Ir_6O_{19}$ (space group $C2/m$) (6), the crystal structure of $Ba_7Ir_6O_{19}$ was used as the initial structure model for refinement based on the X-ray diffraction powder data. The Sr and Re atoms occupy Ba and Ir atoms positions of the $Ba_7Ir_6O_{19}$ crystal structure, respectively, while the Ir (3) position remains unoccupied. After sequential iterations, good agreement between experimental and calculated patterns was achieved: $R_I = 0.032$, $R_P = 0.058$, $R_{wP} = 0.079$, but some reflections with indices $0k0$ were not fitted well enough. The March-Dollase function was used to take the preferred orientation along the [010] direction into account. The following values of reliability factors were obtained: $R_I = 0.018$, $R_P = 0.050$, $R_{wP} = 0.068$ and a preferred orientation parameter, r, of 0.94(1) (7). The observed, calculated, and difference X-ray diffraction patterns are shown in Fig. 1. The final refinement was carried out with one common thermal parameter for all oxygen atoms. The crystallographic parameters, position parameters, and characteristic interatomic distances for $Sr_7Re_4O_{19}$ are listed in Tables 1, 2, and 3, respectively.

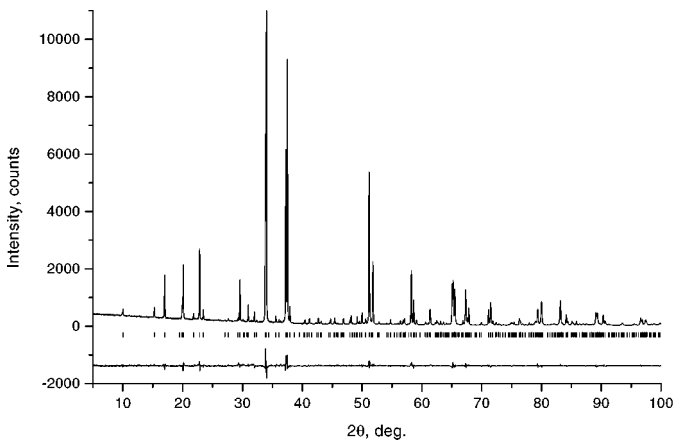

FIG. 1. Experimental, calculated, and difference X-ray patterns for $Sr_7Re_4O_{19}$.

TABLE 1
Crystallographic Parameters for $Sr_7Re_4O_{19}$

Space group	$C2/m$
a (Å)	13.6432(1)
b (Å)	5.60509(5)
c (Å)	10.37483(9)
β	93.3504(5)°
Cell volume (Å^3)	784.97(1)
Z	2
Calculated density (g/cm^3)	7.032
2θ Range (time/step)	5–100°, 90 s
March–Dollase parameter, r[a]	0.94(1)
No. of reflections	340
Refinable parameters	52
Reliability factors	$R_I = 0.018$, $R_P = 0.050$, $R_{wP} = 0.068$

[a] See Ref. (7).

As mentioned above, the $Sr_7Re_4O_{19}$ crystal structure can be derived from the $Ba_7Ir_6O_{19}$ structure (6). The $Ba_7Ir_6O_{19}$ structure consists of units of three face-shared, slightly distorted IrO_6 octahedra. These units are linked together by corner-sharing and form a two-dimensional network in the a/b-plane. Ba atoms have a 10- and 12-fold coordination of oxygen atoms. Note that the $Ba_7Ir_6O_{19}$ structure is closely related to the hexagonal nine-layer $BaRuO_3$ structure (8), which consists of similar units of three face-sharing RuO_6 octahedra. These units build up the three-dimensional network in contrast to the $Ba_7Ir_6O_{19}$ structure. The complex oxide with the proposed composition $Sr_3Re_2O_9$ reported in the literature (3) was suggested to be isostructural with the $Ba_3Re_2O_9$ (4) oxide. Its structure can be derived from the $BaRuO_3$ crystal structure by removing Ru atoms from the middle octahedron of the three face-sharing octahedra units to overcome the electrostatic repulsion between highly

TABLE 2
Positional and Thermal Displacement Parameters for $Sr_7Re_4O_{19}$

Atom	x/a	y/b	z/c	B (Å^2)
Sr(1)	0.7923(3)	0	0.4061(4)	0.5(1)
Sr(2)	0.5839(3)	0	0.1588(4)	0.8(1)
Sr(3)	0.8593(3)	0	0.0470(4)	1.1(1)
Sr(4)	0	$\frac{1}{2}$	$\frac{1}{2}$	0.9(2)
Re(1)	0.0354(2)	0	0.3190(2)	0.99(7)
Re(2)	0.3280(2)	0	0.2164(2)	0.63(6)
O(1)	0.624(1)	0.752(2)	0.376(2)	1.2(1)
O(2)	0.240(1)	0.748(3)	0.157(2)	1.2(1)
O(3)	0.426(1)	0.260(3)	0.287(2)	1.2(1)
O(4)	0.392(1)	0	0.071(2)	1.2(1)
O(5)	0.048(2)	0	0.145(2)	1.2(1)
O(6)	0.690(1)	0	0.610(2)	1.2(1)
O(7)	0	0	$\frac{1}{2}$	1.2(1)

TABLE 3
Characteristic Interatomic Distances (Å) for $Sr_7Re_4O_{19}$

Sr(1)–O(1)	2.65(1) × 2	Sr(4)–O(1)	2.69(2) × 4
	2.78(2) × 2	Sr(4)–O(3)	2.72(2) × 4
Sr(1)–O(2)	2.98(2) × 2	Sr(4)–O(6)	2.70(3) × 2
Sr(1)–O(3)	2.69(2) × 2	Sr(4)–O(7)	2.803 × 2
Sr(1)–O(6)	2.68(3) × 1	Re(1)–O(1)	1.90(1) × 2
	2.818(3) × 2	Re(1)–O(3)	2.00(3) × 2
Sr(1)–O(7)	2.862(4) × 1	Re(1)–O(5)	1.87(2) × 1
Sr(2)–O(1)	2.63(2) × 2	Re(1)–O(7)	2.004(2) × 1
Sr(2)–O(2)	2.53(2) × 2	Re(2)–O(2)	1.92(2) × 2
Sr(2)–O(3)	3.08(2) × 2	Re(2)–O(3)	2.04(2) × 2
Sr(2)–O(4)	2.63(1) × 1	Re(2)–O(4)	1.86(2) × 1
	2.45(2) × 1	Re(2)–O(6)	1.86(2) × 1
Sr(2)–O(5)	2.848(5) × 2		
Sr(3)–O(2)	2.55(2) × 2		
	2.69(2) × 2		
Sr(3)–O(3)	2.86(2) × 2		
Sr(3)–O(4)	2.846(3) × 2		
Sr(3)–O(5)	2.49(3) × 1		
	2.61(3) × 1		

charged neighboring Re^{6+} cations. The crystal structure of $Sr_7Re_4O_{19}$ can be derived from the $Ba_7Ir_6O_{19}$ structure in the same way. It consists of infinite *cis*-bridged chains of the ReO_6 octahedra linked by common corners. Each chain is connected with another one by corner-sharing of each second ReO_6 octahedron. These infinite structure fragments are held together by 10- and 12-coordinated Sr atoms. The projections along the [010] axis of the $Ba_7Ir_6O_{19}$ (a) and the $Sr_7Re_4O_{19}$ (b) crystal structures are shown in Fig. 2. There are two nonequivalent Re positions in the $Sr_7Re_4O_{19}$ crystal structure. As mentioned above Re atoms are situated in distorted octahedra. The average Re–O distance is 1.95 and 1.94 Å for Re(1) and Re(2) atoms, respectively, in good agreement with the ionic radius of Re^{6+} (0.52 Å) for CN = 6. Sr atoms have two different coordinations. Sr(1) and Sr(4) are 12-fold coordinated and Sr(2) and Sr(3) have 10 neighboring oxygen atoms each. The Sr(4) environment is regular in contrast to other Sr/O-polyhedra and can be described as a four capped cube. Other Sr atoms have irregular oxygen coordination. The $Sr_7Re_4O_{19}$ structure may be considered as intermediate between the Ba_2ReO_5 (9) and the $Ba_3Re_2O_9$ (4) structures. The Ba_2ReO_5 compound contains ReO_6 octahedra linked by common corners and form infinite *cis*-bridged chains. In contrast, corner-sharing ReO_6 octahedra build infinite layers in the $Ba_3Re_2O_9$ structure. The $Sr_7Re_4O_{19}$ structure consists of two isolated, infinite chains of corner-sharing ReO_6 octahedra connected with each other. These three different structure motives are shown in Fig. 3.

b. Magnetic Properties of the $Sr_7Re_4O_{19}$

$Sr_7Re_4O_{19}$ shows unexpected magnetic behavior. The temperature dependence of magnetization at a constant field strength of 0.01 T is shown in Fig. 4. These results are in good agreement with the previous investigations of magnetic properties of the reported compound with the proposed composition "$Sr_3Re_2O_9$" (3). This composition corresponds to the mixture of the $Sr_7Re_4O_{19}$ and strontium perrhenate, $Sr(ReO_4)_2$, or its different possible crystallohyd-

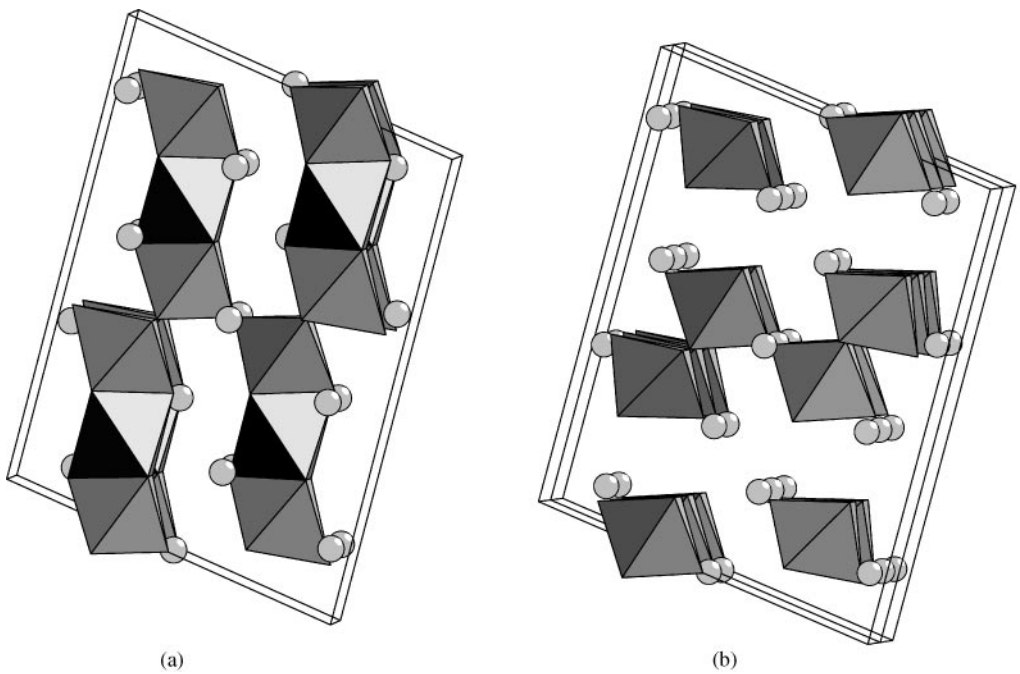

FIG. 2. The projections along [010] axis of $Ba_7Ir_6O_{19}$ (a) and $Sr_7Re_4O_{19}$ (b) crystal structures.

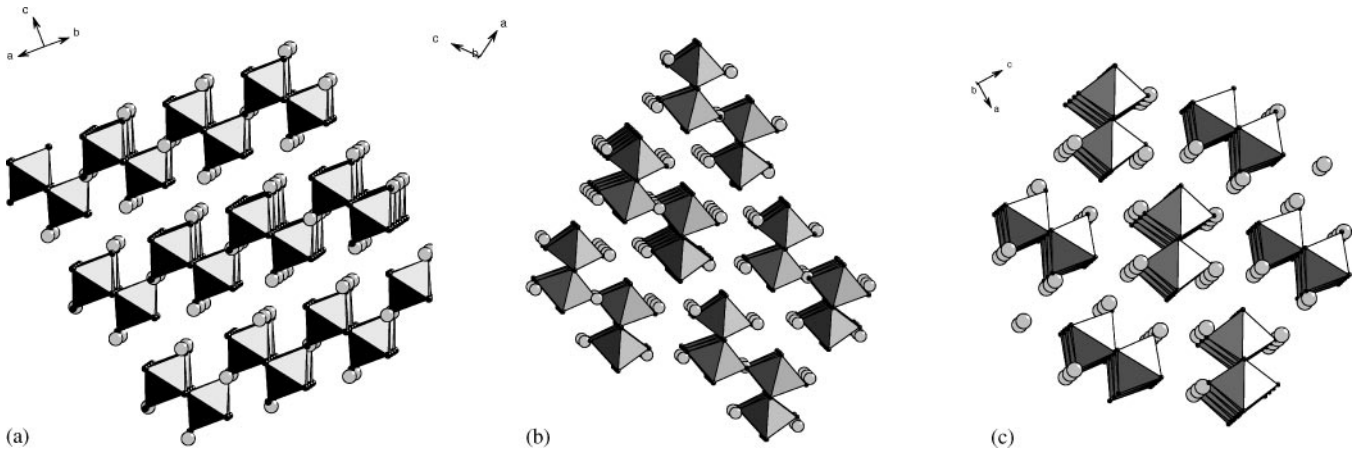

FIG. 3. The main structure motives of $Ba_3Re_2O_9$ (a), $Sr_7Re_4O_{19}$ (b), and Ba_2ReO_5 (c).

rates. Because of diamagnetic behavior of compounds containing rhenium in its highest oxidation state, + 7, the unexpected observed temperature dependence of magnetization may be completely attribute to the $Sr_7Re_4O_{19}$ oxide. Temperature-independent paramagnetism between 80 and 300 K was observed. This unusual magnetic properties of complex rhenium oxide with Re in a low oxidation state, + 6, together with reported semiconducting behavior of "$Sr_3Re_2O_9$" was explained by the delocalization of the $5d^1$ electron in rhenium (VI), since the two-dimensional interactions of vertex-connected octahedra in the structure might be consistent with the electrical properties of "$Sr_3Re_2O_9$" (3). The new knowledge about the $Sr_7Re_4O_{19}$ structure requires for a more detailed study of the magnetic properties of this compound. In addition to the temperature dependence of magnetization further investigations in variable magnetic fields were performed.

The field dependence of magnetization was measured at different temperatures below T_C (see Fig. 5 for $T = 110$ and 300 K). The field dependence can be described by

$$M(H) = M_1(H) + M_2(H), \qquad [1]$$

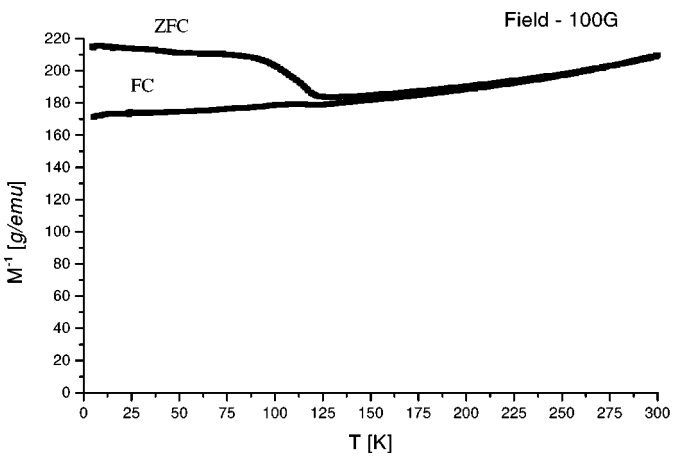

FIG. 4. Temperature dependence of inverse magnetization of $Sr_7Re_4O_{19}$ at constant field strength of 0.01 T.

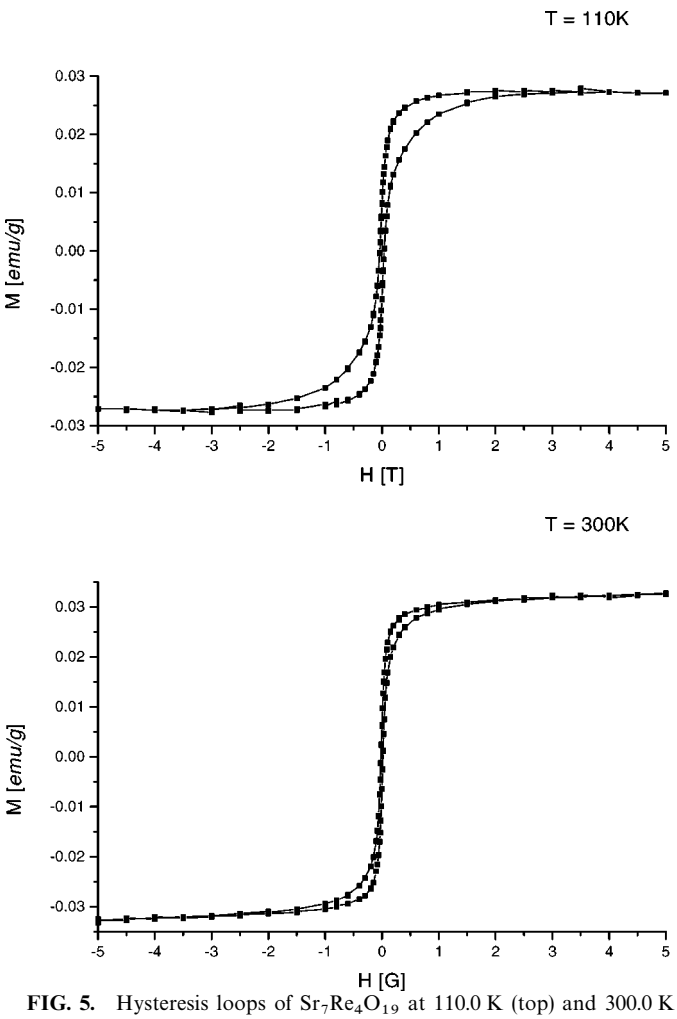

FIG. 5. Hysteresis loops of $Sr_7Re_4O_{19}$ at 110.0 K (top) and 300.0 K (bottom).

TABLE 4
The Field Dependence of Magnetization at Different Temperatures below T_C for $Sr_7Re_4O_{19}$

T(K)	α (10^{-8} emu/(gG))	H_C (G)	H_0 (G)	$\int_{loop} MdH$ ((emuG)/g)	$M_{H\to 0}(\mu_B$ per Re(+6)-ion)
10.0	9.237(6)	660	9960	278	0.00184
50.0	31.33(3)	586	2809	234	0.00176
110.0	−0.944(3)	372	−90042	194	0.00170
150.0	1.807(8)	300	46486	166	0.00168
200.0	2.972(9)	184	30283	114	0.00180
250.0	4.056(6)	175	21696	100	0.00176
300.0	4.498(5)	166	18675	67	0.00168

with

$$M_1(H) = \begin{cases} \alpha\ (H + H_0),\ H \text{ decreasing} \\ \alpha\ (H - H_0),\ H \text{ increasing} \end{cases} \qquad [2]$$

and

$$M_2(H) = \begin{cases} 2\alpha H_0 \tanh[(H + H_C)/\sigma],\ H \text{ decreasing and } H < (H_C), \\ 2\alpha H_0 \tanh[(H - H_C)/\sigma],\ H \text{ increasing and } H > H_C, \\ 0, \text{ else.} \end{cases} \qquad [3]$$

Four parameters, α, H_0, σ, and H_C, have to be fitted to the observed data points. The results are given in Table 4. The areas within one complete loop are calculated according to Eq. [3] with the parameters given in Table 4.

ACKNOWLEDGMENTS

This work was supported by BMBF (Bundesministerium fuer Bildung und Forschung). Authors thank G. Miehe for carefully performed electron microscope study and R. Theissmann for the help with the SQUID measurements.

REFERENCES

1. G. Baud, J. P. Besse, R. Chevalier, and B. L. Chamberland, *J. Solid State Chem.* **28,** 157 (1979).
2. K. G. Bramnik, G. Miehe, H. Ehrenberg, H. Fuess, A. M. Abakumov, R. V. Shpanchenko, V. Yu. Pomjakushin, and A. M. Balagurov, *J. Solid State Chem.* **149,** 49 (2000).
3. B. L. Chamberland and F. C. Hubbard, *J. Solid State Chem.* **26,** 79 (1978).
4. C. Calvo, H. N. Ng, and B. L. Chamberland, *Inorg. Chem.* **17,** 699 (1978).
5. F. Izumi, in "The Rietveld Method" (R. A. Young, Ed.), Chap. 13. Oxford Univ. Press, Oxford, 1993.
6. C. Lang and H. Mueller-Buschbaum, *Monatsh. Chem.* **120,** 705 (1989).
7. W. A. Dollase, *J. Appl. Crystallogr.* **19,** 267 (1986).
8. P. C. Donohue, L. Katz, and R. Ward, *Inorg. Chem.* **4,** 306 (1965).
9. A. K. Cheetham and D. M. Thomas, *J. Solid State Chem.* **71,** 61 (1987).